Trends in Applied Sciences Research

ISSN 1819-3579

Academic
Journals Inc.

www.academicjournals.com

Trends in Applied Sciences Research 6 (12): 1335-1344, 2011
ISSN 1819-3579 / DOI: 10.3923/tasr.2011.1335.1344

Large Signal Analysis of Spatial Chirped Grating Distributed Feedback Laser

[1]Masoud Jabbari and [2]Ghahraman Solookinejad
[1]Department of Electrical Engineering, Islamic Azad University, Marvdasht Branch, Marvdasht, Iran
[2]Department of Physics, Islamic Azad University, Marvdasht Branch, Marvdasht, Iran

Corresponding Author: Masoud Jabbari, Department of Electrical Engineering, Islamic Azad University, Marvdasht Branch, Marvdasht, Iran

ABSTRACT

Lasers play an important role in all optical communication systems. One of the influential laser sources is Distributed Feedback (DFB) laser. In this study, based on the coupled wave and carrier rate equations a spatial chirped grating distributed feedback laser has been simulated and investigated. Also, the effects of some parameters including spatial chirped grating, kappa L and phase shift on the large signal output power responses has been investigated. The results showed to had a single mode, high Side Mode Suppression Ratio (SMSR) and high optical output power. The parameters such as chirp coefficient and injection current have been adjusted about 1.5×10^{-3} and 200 mA, respectively. By adjusting the chirped coefficient and injection current and using the $\lambda/4$ phase shift in the middle of the DFB laser, the output optical power was single mode. Also, side mode suppression ratio and optical output power were more than 50 dB and 60 mW, respectively. Therefore by optimizing the parameters such as injection current, amount of spatial chirped grating and phase shift, a DFB laser with high output power and high SMSR have been achieved. The simulation was based on the Finite Difference Time Domain (FDTD) numerical method.

Key words: Distributed feedback, finite difference time domain, coupling coefficient, spatial chirped grating, phase shift

INTRODUCTION

Nowadays, optical communication systems play a key role in computer networks, optical receivers using conventional sub-micron CMOS technology, image transfer and people communication (Temmar and Belghoraf, 2006; Asadpour and Golnabi, 2008; Touati *et al*., 2007). In order to increase operational speed in optical communication systems, all-optical devices should be used. Lasers are one of the most applicable devices that act as sources for optical communications, robot and camera network, wheat germination and optical elements (Chu *et al*., 2011; Agrawal, 2002; Abu-Elsaoud *et al*., 2008; Liang *et al*., 2010).

In some applications, for example when fiber loss became vital or in a system that coherent detection techniques are used, operation of laser as a single frequency source with high power is necessary. There are some ways to provide single mode operation. The way that is commonly used, is periodic structures. Distributed Feedback (DFB) laser (Shahshahani and Ahmadi, 2008; Bazhdanzadeh *et al*., 2008; Morgado *et al*., 2010) and Distributed Bragg Reflector (DBR) laser (Signoret *et al*., 2004) are two types of applicable structures. In DBR lasers, active region and

spatial grating are longitudinally separated. But in DFB laser these two sections are combined. Fabrication of DFB lasers is simpler than DBR lasers because of longitudinally uniform structure. Instead, DFB analysis is more complicated as a result of dependency between gain and phase condition. Many DFB structures are fabricated with uniform grating in laser section to achieve maximum optical output power. Sometimes laser characteristics including Side Mode Suppression Ratio (SMSR), lasing wavelength and optical output power are unstable because of phase uncertainty in grating at the facets. As a result, although the device is fabricated on the same wafer, transform operation of conventional DFB lasers with uniform grating changes (Bazhdanzadeh *et al*., 2008).

To obtain a single mode source power, in some structures, grating of DFB laser has a $\lambda/4$ phases shift in the middle of device. In uniform grating DFB diode lasers, there is a limit to increase coupling coefficient (κL); because in high coupling coefficient, Longitudinally Spatial Hole Burning (LSHB) causes spectral instability. But, $\lambda/4$ phase shifted DFB lasers operate in single mode even though with relatively large κL. This is another advantage of DFB laser with $\lambda/4$ phase shift. Also, when putting in combined structures with modulator, DFB lasers large κL have high immunity against optical feedback caused by facets reflections (Jia *et al*., 2007).

To overcome these problems, inserting spatial grating chirp in distributed feedback laser structure is another way to improve its output parameters such as power, SMSR and single mode output power (Hillmer *et al*., 2004). So in this study, first we have simulated the conventional DFB laser and also have compared their results with the other studies. Then, by using the mentioned results, the effects of spatial chirped grating on the dynamic large signal response is investigated.

DFB LASER STRUCTURE

In order to study the fundamental characteristics of a DFB laser, a DFB-laser has been considered to be uniform (conventional) and non-uniform (linear chirp) grating operating at 1550 nm. The device structure and its parameters, used in simulation, are shown in Fig. 1 and Table 1, respectively. The model structure is assumed to be a traveling-wave type DFB laser with no facets reflections merely supporting a single transverse mode.

Furthermore, the current is considered to be uniformly injected into the entire area of the device, while the local carrier densities vary with position in the active region. Thus, the carrier density in each section can be derived from the corresponding rate equations.

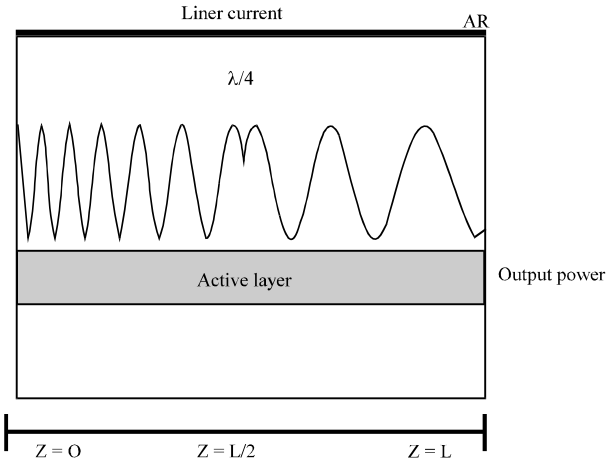

Fig. 1: Schematic model of a DFB laser structure and operational configuration

Table 1: Device parameters used in simulation

Symbol	Description	Value
L	Active region length	300 μm
W	Active region width	2 μm
d	Active region thickness	0.15 μm
Γ	Optical confinement factor	0.32
a_m	Linewidth enhancement factor	4.89
N_0	Carrier density at transparency	$1.5\times10^{24}m^3$
n	Modal refractive index	3.2353
σ	Mode cross section	10^{-12} m^2
κL	Coupling coefficient	2.5
$R_1 = R_2$	Facets Reflectivities	0
Anrad	Nonradiative recombination constant	1×108 sec^{-1}
B_{rad}	Radiative recombination constant	2.5×10^{-17} $m^3 sec^{-1}$
C_{Aug}	Auger recombination constant	9.4×10^{-41} m^6 sec^{-1}
a_1	Material gain constant	6×10^{-20} m^2
a_2	Material gain constant	7.4×10^{18} m^{-3}
a_3	Material gain constant	3.115×10^{25} m^4
a_4	Material gain constant	3.0×10^{-32} m^{-4}
λ_0	Wavelength at transparency	1550 nm

GENERAL FORMALISM

The time-domain traveling wave model based on the coupled wave equations is well established for simulating DFB structures. In the spatial domain, such devices exhibit nonuniform carrier and photon distributions along the propagation direction. Therefore, the governing equations have to be discretized along the active layer in a DFB laser, to treat these variations. Obviously, these equations and the discretization scheme can also be adopted to describe the processes in DFB laser. DFB structures are normally designed for single-mode operation. Therefore, it is sufficient that the governing equations are solved only in a narrow spectral range near the lasing wavelength, where the phase information is preserved. The electric field in this type of waveguide is expressed as:

$$E(x,y,z,t) = \varphi(x,y)[F(z,t)e^{-j\beta_0 z} + R(z,t)e^{j\beta_0 z}]e^{j\omega_r t} \tag{1}$$

where, $\beta_0=\pi/\Lambda$ is the propagation constant at the Bragg wavelength, Λ is the grating period, ω_r is the reference frequency and $\varphi(x,y)$ is the transverse field profile. F(z,t) and R(z,t) represent the complex electrical field envelopes of forward and backward traveling waves, respectively. Substitution of Eq. 1 into Maxwell's equations yields the following time-dependent coupled wave equations governing the lasing mode field propagating in the DFB laser active layer (Jabbari *et al*., 2009):

$$\frac{1}{v_g}\frac{\partial F(z,t)}{\partial t} + \frac{\partial F(z,t)}{\partial z} = \left\{-j\delta_0 + \frac{1}{2}\left(\Gamma g_m(z,t) - \alpha_s\right)\right\}F(z,t) + j\kappa R(z,t) + s_{(f)}(z,t) \tag{2a}$$

and:

$$\frac{1}{v_g}\frac{\partial R(z,t)}{\partial t} - \frac{\partial R(z,t)}{\partial z} = \left\{-j\delta_0 + \frac{1}{2}\left(\Gamma g_m(z,t) - \alpha_s\right)\right\}R(z,t) + j\kappa F(z,t) + s_{(r)}(z,t) \tag{2b}$$

where, v_g is the group velocity, α_s accounts for internal loss which is assumed to be negligible, κ denotes the grating coupling coefficient and s_r and s_f represent the spontaneous emission noise and will be simulated by a Gaussian-distributed random number generator satisfying the condition (Park *et al*., 2003):

$$\left\langle s_{(f,r)}(z,t,\lambda_k)s^*_{(f,r)}(z',t',\lambda_{k'})\right\rangle = \gamma\frac{R_{sp}(z,t,\lambda_k)}{Lv_g}\times\delta(z-z')\delta(t-t')\delta(\lambda_k-\lambda_{k'})$$

where, L is the length of the active section and γ is the coupling coefficient of the spontaneous emission rate R_{sp} into the waveguide. The expression for R_{sp} will be given later in our optical gain model. The phase detuning factor from the Bragg wavelength is given as (Jabbari *et al*., 2009):

$$\delta_0 = \beta(\lambda_s) + \frac{1}{2}\alpha_m g_m(z,t) - \beta_0 \tag{3}$$

where, $\beta(\lambda_s) = 2\pi n_{eff}/\lambda_s$ is the signal wave propagation constant and λ_s is the signal wavelength, a_m denotes the linewidth enhancement factor and $g_m(z,t)$ is the material gain which depends on the carrier density, N(z, t) and wavelength.

In the non-uniform DFB laser the variations in the period of the grating are small. So, the coupled-mode Eq. 2a and 2b remain unaltered except for the detuning parameter d which now depends on z. For a linear spatial chirp, detuning factor is given by (Jabbari *et al*., 2009):

$$\delta(z)L = \delta_0 L - C(z-L/2)/L \tag{4}$$

where, δ_0 is the constant phase detuning which should be smaller than that for which the Bragg resonances occur, as for the uniform DFB laser and C is the chirp parameter. In order to model the asymmetric gain profile, the gain spectrum is assumed to be cubic and the material gain is approximately by Jabbari *et al*. (2009):

$$g_{m,i} = g_m(N_i,\lambda s) = a_1(N_i-N_0) - a_2(\lambda s-\lambda_N)^2 + a_3(\lambda s-\lambda_N)^3 \tag{5}$$

where, a_1, a_2 and a_3 are gain constant and N_0 is the carrier density at transparency for the peak wavelength λ_N, which is assumed to shift linearly with the carrier density , i.e., $\lambda_N = \lambda_0 - a_4(N-N_0)$, with λ_0 and a_4, being the peak wavelength at transparency and gain constant. Neglecting the facets reflectivity coefficients (i.e., $R_1 = R_2 = 0$), the boundary conditions reduce to:

$$F(0,t) = E_{in}(0,t) \tag{6a}$$

$$R(L,t) = E_{in}(L,t) \tag{6b}$$

where, E_{in} is the input optical field. In an active layer whose thickness (d) and width (W) are both much larger than the carrier diffusion length, the rate equation for the carrier density becomes:

$$\frac{\partial N(z,t)}{\partial t} = \frac{J}{qd} - \frac{N(z,t)}{\tau_c} - \Gamma\frac{\sigma}{\hbar Wd}\sum_{k=s}\left(\frac{g_m(z,t)|P_s(z,t)|^2}{\omega_s}\right) \tag{7}$$

where, J = I/(WL) is the current density, L is the active region length, σ is the mode cross section and τ_c is the carrier life time:

$$\tau_c = \{A_{nard}+B_{rad}N(z,t)+C_{Aug}N^2(z,t)\}^{-1} \quad (8)$$

where, A_{nrad} is the nonradiative recombination rate due to Shockley-Read-Hall (SRH) process, B_{rad} is the total radiative recombination rate and C_{Aug} is the total Auger recombination rates.

SIMULATION

Finite difference time domain is one of the powerful method to analyze all optical active and passive devices and photonic crystal such as optical filter, optical coupler and waveguide bending, (Dekkiche and Naoum, 2007, 2008; Djavid *et al*., 2008). In this study, the performance of DFB laser with uniform and nonuniform gratings, using FDTD method have been simulated. As a starting point, by solving the carrier density rate equation in each section, (z,t) have been obtained. This has allowed us to calculate the material gain coefficient, g_m, in the corresponding section. Then, it is assumed that the duration of the input pulse is much longer than the round-trip time in the cavity. Such an assumption has enabled us to ignore the spatial derivative term in eq. 2. Then, to solve for the forward and backward waves by FDTD method, with an appropriate accuracy, the length, L, have been divided into M = 30 equal sections. It is also assumed that the distribution of carrier and photon densities in each section to be uniform and have applied Lax average technique to the time dependent coupled wave equations (Carroll *et al*., 1998). Thus:

$$\begin{aligned} F_{z+1}^{T+1} &= AF_z^T + BR_{Z+1}^T + C1s_f + C2s_r \\ R_z^{T+1} &= DF_z^T + ER_{z-1}^T + G1s_f + G2s_r \end{aligned} \quad (9)$$

where, T and Z are the time and length steps, respectively, while the coefficients A, B, D, E, C_1 and C_2 are:

$$A = E = \frac{1}{\Delta}\left(\left(L^2 - \left(\frac{gL - j\delta L}{2}s\right)^2\right) - \left(\frac{\kappa Ls}{2}\right)^2\right) \quad (10a)$$

$$B = D = \frac{1}{\Delta}\left(\left(L - \frac{gL - j\delta L}{2}s\right)\left(\frac{j\kappa Ls}{2}\right) + \left(\frac{j\kappa Ls}{2}\right)\left(L + \frac{gL - j\delta L}{2}s\right)\right) \quad (10b)$$

$$C1 = G2 = \frac{1}{\Delta}\left(L - \frac{gL - jdL}{2}s\right)Ls \quad (10c)$$

$$C2 = G1 = \frac{1}{\Delta}\left(\frac{jkLs}{2}\right)Ls \quad (10d)$$

where, s = L/M is the length of each section and:

$$\Delta = \left(L - \frac{s}{2}(gL - j\delta L)\right)^2 + \left(\frac{\kappa Ls}{2}\right)^2 \quad (11)$$

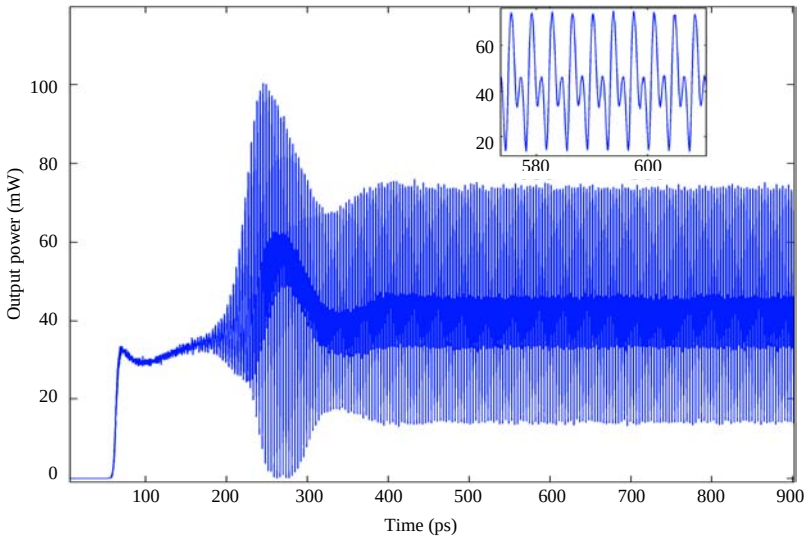

Fig. 2: Optical output power versus time from the emission facet in the DFB laser. (insert: mode beating). Injection current is the above threshold condition (42.5 mA)

In order that to compare the results, the parameters such as coupling coefficient, length, spatial chirp coefficient and injection current are chosen κL = 2.5, 300 μm, 1.5×10^{-3} and 90 mA, respectively. The other required structural parameters are given in Table 1.

By adjusting the injection current above threshold condition, the optical output powers from the both facets begin to lasing. As is shown in the Fig. 2, optical output power versus time from the emission facet of the conventional DFB laser is plotted. Lasing starts after passing needed time to satisfy the threshold condition. But output power does not have specific amount because of modes beating. To show the effects of modes beating in the optical output power responses, part of output power is given in the right up corner of the Fig. 2, in which existence of different frequencies is obvious. In other words, laser does not operate as a single frequency source. The output power spectrum is shown in Fig. 3. There are side modes in addition to the main one. Side mode's amplitudes are comparable to the main mode ones and they cannot be ignored. Hence, laser moves among side mode's peaks continuously.

The effects of spatial hole burning in the DFB lasers make local variations in the carrier density and hence variations in real refractive index and gain, give rise to change in magnitude and phase of the feedback from each section of the grating. Hence, the longitudinal mode intensity distribution and also alters the gain suppression of side modes relative to the lasing mode are changed. The lasing mode then exhibits a nonlinear light/current characteristic which is accompanied by a frequency shift or chirp.

As is shown in Fig. 4, spatial hole burning changes the magnitude of the forward, backward and total internal power along the length of waveguide. At the middle of the cavity, spatial hole burning causes reduction in the carrier density and hence, carrier density at the middle of cavity is decreased relative to the facets. Therefore, internal optical power increase at the middle of the DFB laser and decrease at the facets as is shown in Fig. 4.

However, to have a single mode operation laser and to increase the optical output power, the effect of hole burning should be minimized. One way to achieve single mode output power, is

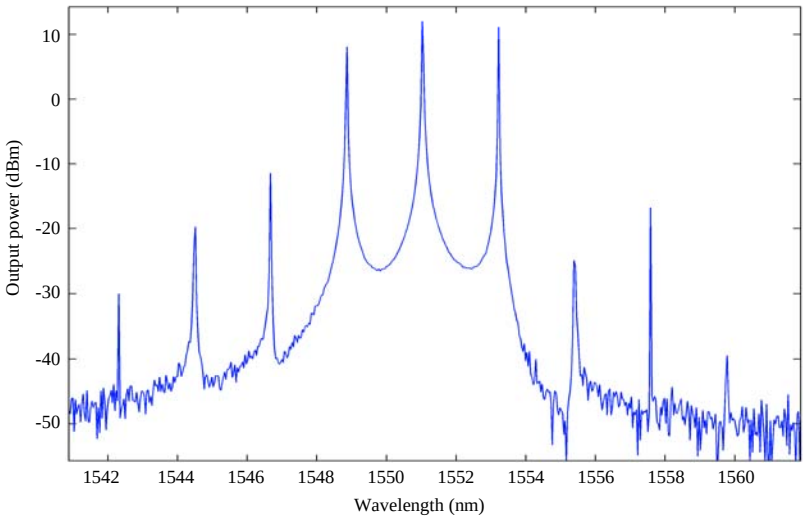

Fig. 3: Optical output power versus wavelength of the conventional DFB laser without phase shift in the middle of device. Injection current is adjusted about 42.5 mA above the threshold condition

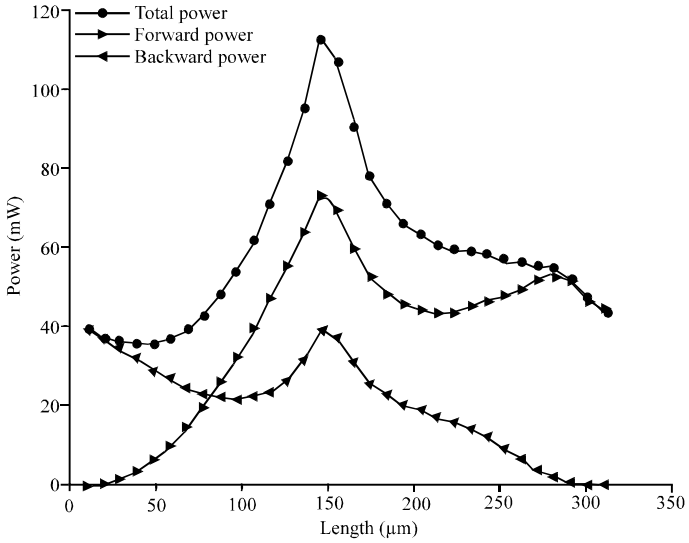

Fig. 4: Output power versus length of waveguide of conventional DFB laser

inserting λ/4 phase shift in the middle of the device or spatial chirp into the grating structure. So, the DFB laser with λ/4 phase shift and spatial chirp grating is simulated. To compare the results, the other structural parameters are kept the same as previous structure. To show the effects of λ/4 phase shift and spatial chirp grating in the DFB laser on the responses, optical output power versus time is plotted in Fig. 5. The structure has a specific output power in its stable situation. The reason is that, in one hand the reflection of optical wave experience higher feedback toward the rear facet and lower feedback toward emission facet and on the other hand the λ/4 phase shift in the middle of the DFB laser reduce the optical power in the middle of device and hence the laser acts as a

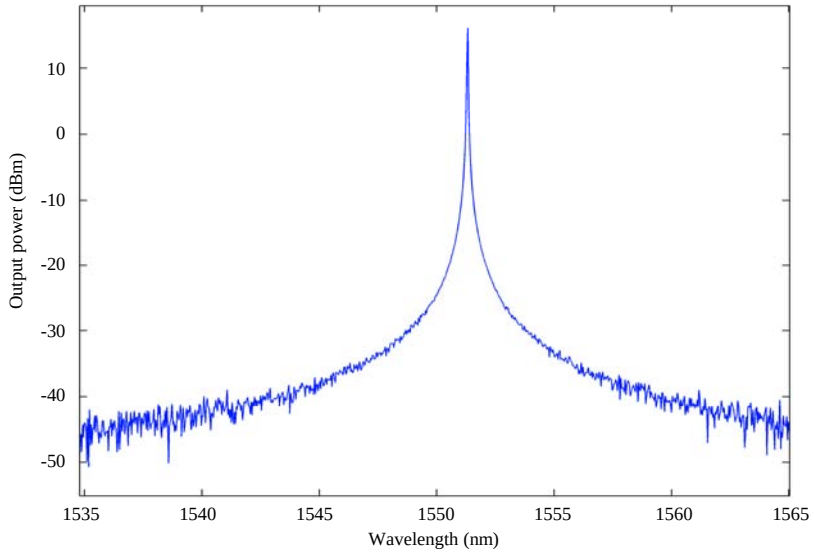

Fig. 5: Large signal output power versus time in the spatial chirped grating DFB laser with λ/4 phase shift in the middle of device. Injection current is the same as conventional DFB laser

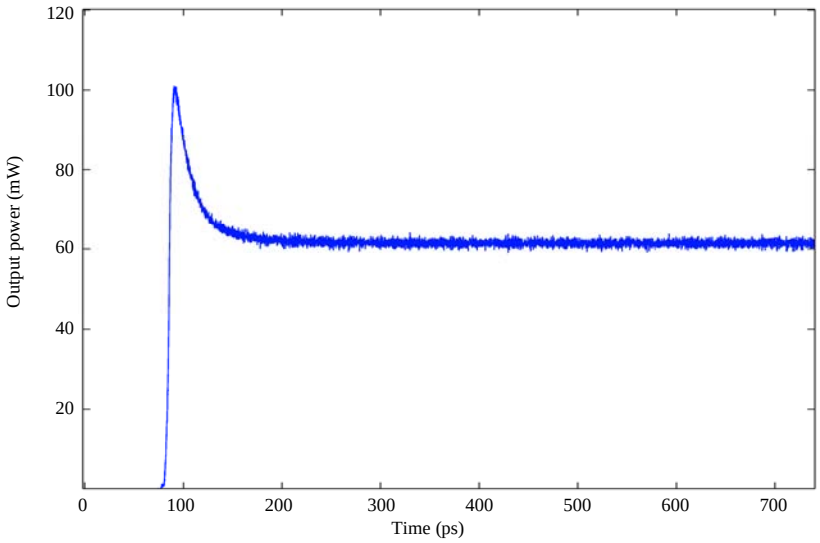

Fig. 6: Optical output power versus wavelength of the spatial chirped grating DFB laser with λ/4 phase shift in the middle of device

single mode source and there isn't any side mode in the spectrum as is shown in the Fig. 6. Furthermore side mode suppression ratio (SMSR) is more than 60 dB due to the single mode output power.

Finally, to show the effects of the spatial chirped grating and phase shift on the DFB laser the carrier density and forward, backward and total internal power have been plotted versus DFB laser length along the waveguide in the Fig. 7a and b, respectively. Due to the reduction of

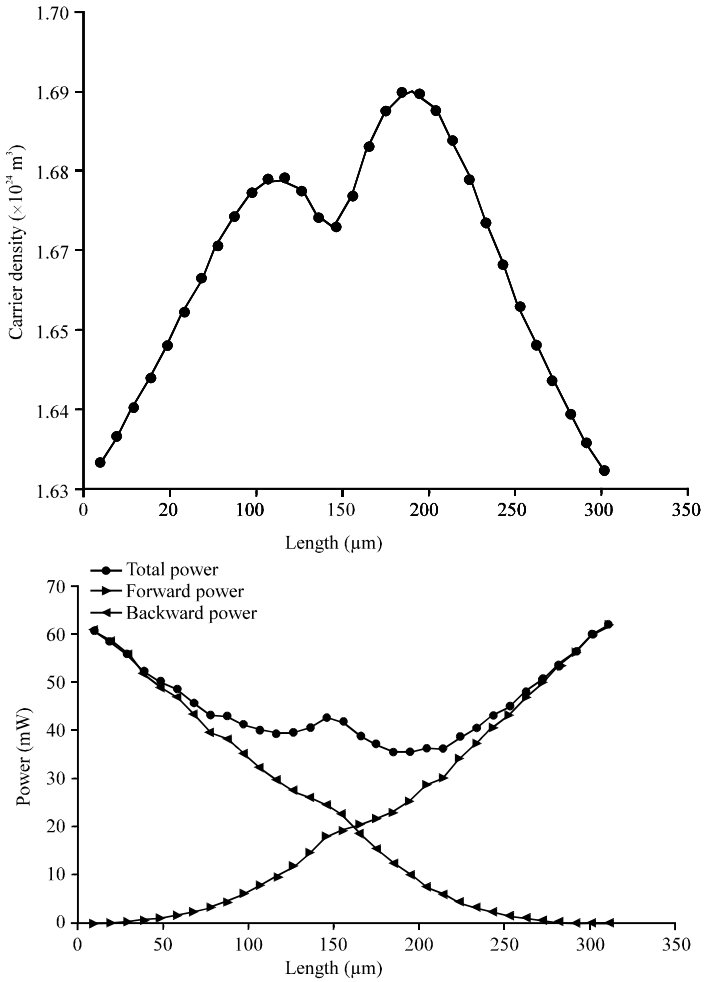

Fig. 7: (a)Carrier density and (b) forward, backward and total internal power along the spatial chirped grating DFB laser with $\lambda/4$ phase shift

spatial hole burning, carrier density is maximum at the center and minimum at the facets as is shown in Fig. 7a. Output power is increased by reduction in carrier density at the facets. Hence, optical output power is increased (about 60 mW) relation to the uniform structure (42.5 mW).

CONCLUSION

The results of simulation show that in uniform DFB laser with high κL, DFB laser is not in single mode operation because optical output laser oscillate between both modes near the Bragg wavelength. Hence, by adding λ/λ 4 phase shift and spatial chirp into the grating structure, DFB laser acts as a single frequency source and output power and SMSR will be more than 50 mW and 60 dB, respectively.

REFERENCES

Abu-Elsaoud, A.M., S.T. Tuleukhanov and D.Z. Abdel-Kader, 2008. Effect of infra-red laser on wheat (*Triticum aestivum*) germination. Int. J. Agric. Res., 3: 433-438.

Agrawal, G.P., 2002. Fiber-Optic Communication Systems. 3rd Edn., John Wiley and Sons Inc., Canada.

Asadpour, A. and H. Golnabi, 2008. Beam profile and image transfer study in multimode optical fiber coupling. J. Applied Sci., 8: 4210-4214.

Bazhdanzadeh, N., V. Ahmadi, H. Ghafoorifard and F. Shahshahani, 2008. Dynamic response of QWS-DFB lasers with convex tapered grating structure and non-zero facet reflection. Solid-State Electron., 52: 221-226.

Carroll, J., J. Whiteaway and D. Plumb, 1998. Distributed Feedback Semiconductor Lasers. Institution of Electrical Engineers, London, ISBN: 9780852969175, Pages: 412.

Chu, H., Z. Xie, X. Xu, L. Zhou and Q. Liu, 2011. Inspection and recognition of generalized surface defect for precise optical elements. Inform. Technol. J., 10: 1395-1401.

Dekkiche, L. and R. Naoum, 2007. A novel all-optical switch based on a photonic crystal coupler. J. Applied Sci., 7: 3518-3523.

Dekkiche, L. and R. Naoum, 2008. Optimal design of 90° bend in two dimensional photonic crystal waveguides. J. Applied Sci., 8: 2449-2455.

Djavid, M., A. Ghaffari, F. Monifi and M. S. Abrishamian, 2008. Photonic crystal narrow band filters using biperiodic structures. J. Applied Sci., 8: 1891-1897.

Hillmer, H., C. Prott, F. Romer and S. Hansmann, 2004. Theoretical model calculations of long-haul edge-emitting communication lasers: Comparison of fractally mixed, fine-pitched and continuously chirped DFB gratings. Semicond. Sci. Technol., 19: 939-945.

Jabbari, M., M.K. Moravvej-Farshi, R. Ghayour and A. Zarifkar, 2009. XPM response of a chirped DFB-SOA all-optical flip-flop injected with an assist light at transparency. Lightwave Technol. J., 27: 2199-2207.

Jia, X.H., D.Z. Zhong, F. Wang and H.T. Chen, 2007. Dynamic single mode and modulation characteristics analysis for phase shifted distributed feedback lasers with chirped grating. Opt. Commun., 279: 356-363.

Liang, Z., X. Ma, F. Fang and S. Zhu, 2010. Improved Monte Carlo localization algorithm in a hybrid robot and camera network. Inform. Technol. J., 9: 1585-1597.

Morgado, J.A.P., C.A.F. Fernandes and J.B.M. Boavida, 2010. Novel DFB laser structure suitable for stable single longitudinal mode operation. Optics Laser Technol., 42: 975-984.

Park, J., X. Li and W.P. Huang, 2003. Performance simulation and design optimization of gain-clamped semiconductor optical amplifiers based on distributed bragg reflectors. IEEE J. Quantum Electron., 39: 1413-1423.

Shahshahani, F. and V. Ahmadi, 2008. Analysis of relative intensity noise in tapered grating QWS-DFB laser diodes by using three rate equations model. Solid-State Electron., 52: 857-862.

Signoret, P., M. Myara, J.P. Tourrenc, B. Orsal and M.H. Monier *et al*., 2004. Bragg section effects on linewidth and lineshape in 1.55 μm DBR tunable laser diodes. IEEE Photonics Technol. Lett., 16: 1429-1431.

Temmar, A. and A. Belghoraf, 2006. Radiation spectral integral for tapered structure in optical communication. Inform. Technol. J., 5: 719-725.

Touati, F., S. Douss, N. Elfadil, Z. Nadir, M.B. Suwailam and M. Loulou, 2007. High-performance optical receivers using conventional sub-micron CMOS technology for optical communication applications. J. Applied Sci., 7: 559-564.